Effect of a product on spontaneous droplet motion driven by a chemical reaction of surfactant

Takahiro Tanabe [1] Takuto Ogasawara,[2] and Nobuhiko J. Suematsu [1,2,*]

[1]*Meiji Institute for Advanced Study of Mathematical Sciences (MIMS), Meiji University, 4-21-1 Nakano, Nakano-ku, Tokyo 164-8252, Japan*
[2]*Graduate School of Advanced Mathematical Sciences, Meiji University, 4-21-1 Nakano, Nakano-ku, Tokyo 164-8525, Japan*

We focus on the self-propelled motion of an oil droplet within an aqueous phase or an aqueous droplet within an oil phase, which originates from an interfacial chemical reaction of surfactant. The droplet motion has been explained by mathematical models, which require the assumption that the chemical reaction increases the interfacial tension. However, several experimental reports have demonstrated self-propelled motion with the chemical reaction decreasing the interfacial tension. Our motivation is to construct an improved mathematical model, which explains these experimental observations. In this process, we consider the concentrations of the reactant and product on the interface and of the reactant in the bulk. Our numerical calculations indicate that the droplet potentially moves in the cases of both an increase and a decrease in the interfacial tension. In addition, the reaction rate and size dependencies of the droplet speed observed in experiments were well reproduced using our model. These results indicate the potential of our model as a universal one for droplet motion.

I. INTRODUCTION

Interfacial chemical reaction generates variety of interesting phenomena, e.g., convection and fingering pattern formation [1–3], self-division of droplets [4], growing chemical gardens [5], and self-propelled droplets. There are many reports on self-propelled objects moving on a liquid-solid interface or in a liquid phase [6–11]. For example, a solid disk or liquid droplet can potentially show spontaneous motion on a water surface [12–19]. Although the substances from which these objects are composed are different for each experiment, they all decrease the surface tension of water by dissolving surfactant molecules from the object [7]. In addition, these molecules are removed from the water surface by sublimation and/or dissolution, which forms a concentration gradient on the water surface resulting in a surface tension gradient. The ideal symmetric profile is broken by small fluctuations, which generate a driving force on the object toward the lower-concentration region, i.e., higher-surface-tension region. The asymmetric profiles of the concentration and surface tension around the object are further enhanced by its movement, namely, the object continues to move. These spontaneous motions are also observed in an oil droplet sliding on a solid plate in a surfactant solution [20–25]. In this case, the hydrophobicity of the plate increases with time due to the adsorption of the surfactant and decreases due to desorption from the plate into the oil droplet. In both cases, spontaneous motion originates from the imbalance between the concentration fields coupled with the object motion.

We now focus on the self-propelled motion of an oil droplet in an aqueous phase or an aqueous droplet in an oil phase, which originates from an interfacial chemical reaction of the surfactant [26–31]. The droplet motion is phenomenologically understood as follows. The surfactant adsorbs onto the oil/aqueous interface homogeneously, and an interfacial chemical reaction occurs. At this point, once small fluctuations break the homogeneous surfactant distribution, Marangoni flow is generated on the interface due to the interfacial tension gradient. If the flow enhances the initial fluctuation, the amplitude of the inhomogeneity increases with time, i.e., a positive feedback process occurs, and this results in steady flow, which drives the droplet stably. The question is how the flow enhances the initial fluctuation.

Several mathematical models have been developed to answer this question. Thutupalli *et al.* suggested a simple mathematical model focusing on the surface concentrations of the surfactants, which are both the reactant and the product of the interfacial chemical reaction [28]. In this model they assumed that the sum of the surface concentrations of the reactant and the product is homogeneous in space and constant in time. Namely, the chemical reaction changes only the ratio of the reactant and product. Marangoni flow is generated toward the region of higher interfacial tension. Thus, if the interfacial chemical reaction increases interfacial tension, the flow carries the products to the region with a high product ratio. However, in the opposite case, the initial fluctuation is suppressed. Therefore, the droplet motion requires that the chemical reaction of the surfactant increases the interfacial tension. The experimental system had also been modeled by Schmitt and Stark based on the diffusion-advection-reaction equation for the covering density difference between the product and the reactant at the interface [32]. The basic setup of this model is similar to the Thutupalli model, and thus, the Schmitt model also required the increase of interfacial tension for the droplet motion.

Another mathematical model was suggested by Yoshinaga *et al.*, in which both the bulk and interfacial concentrations of the surfactant were considered and a decomposition

---

*Also at Graduate School of Advanced Mathematical Sciences, Meiji University; suematsu@meiji.ac.jp

reaction of the surfactant was assumed [33]. In this case, due to the decomposition reaction, the surfactant concentration in the bulk decreases in the vicinity of the droplet. If the droplet is slightly perturbed, the bulk concentration profile is distorted. In this time, the bulk concentration around the droplet increases in the direction of motion, which we call here the front, and that in the opposite direction decreases. Therefore, the interfacial tension decreases further in the front direction, and Marangoni flow is generated from the front to the back. This flow propels the droplet in the same direction as the initial perturbation because of momentum conservation. Hence, the initial perturbation increases with time and the droplet continuously moves. In this case, the decomposition reaction at the interface increases the interfacial tension. Namely, based on both of the mathematical models suggested previously, the interfacial chemical reaction must increase interfacial tension for the droplet motion. However, there are several experimental reports that demonstrate evidence of the opposite.

One example is a nitrobenzene droplet including di(2-ethylhexyl) phosphoric acid (DHEPA), which spontaneously swims in a high-pH aqueous phase where a deprotonation reaction of DHEPA occurs on the interface [29]. The equilibrium interfacial tension decreases with an increase in the surface concentration of deprotonated DHEPA. Namely, the chemical reaction decreases the interfacial tension. The droplet, however, spontaneously moves. Another example is observed in an aqueous droplet of a bromine solution swimming in a squalane oil phase including the surfactant monoolein (MO) [28]. In this case, bromination of MO drives the droplet motion. Systematic measurement of the time series of interfacial tension revealed that the bromination reaction decreases the interfacial tension [34]. The droplet, however, spontaneously moves.

This conflicting experimental evidence demands modification of the mathematical model for a self-propelled droplet driven by an interfacial chemical reaction. Here we modify the Yoshinaga model to construct an alternative mathematical model. As we phenomenologically explain above, the essence of the Yoshinaga model is that the profile of the surfactant concentration in the bulk drives the droplet motion. In fact, in the case of the original Yoshinaga model, the chemical reaction increases the interfacial tension. However, this is a collateral effect originating from the decomposition reaction. Thus, if we consider a chemical reaction other than the decomposition reaction, it may not be a necessary condition that the chemical reaction increases interfacial tension. To verify the above hypothesis, we additionally consider the effect of the product of the interfacial chemical reaction. We expect the improved model to lead to a universal understanding of self-propelled objects.

II. MATHEMATICAL MODEL

A. Model

We now modify the Yoshinaga model [33] to expand the phenomenological explanation of spontaneous droplet motion to cover various kinds of chemical reactions. In particular, our purpose is to discuss the droplet motion that occurs when the interfacial tension decreases after a chemical reaction. Namely, we aim to additionally consider the effect of the product induced by the chemical reaction. We consider an axisymmetric droplet system in the bulk, which has a surfactant concentration $c(r, \theta)$ and velocity field $\vec{v}(r, \theta) = (v_r(r, \theta), v_\theta(r, \theta))$ in the comoving frame with the droplet. Several assumptions are incorporated into our model, including that there are two kinds of surfactants at the interface, reactant $\Gamma_1(\theta)$ and product $\Gamma_2(\theta)$. The adsorption of the reactant is expressed by the diffusion coefficient D, and the product Γ_2 is induced by the chemical reaction with reaction coefficient κ_2. Because of the low concentration of the product in the bulk, adsorption of the products is negligible. There are no surfactants in the droplet due to their low solubility. A linear relationship between the interfacial tension γ and the interfacial concentrations Γ_1 and Γ_2 is assumed as $\gamma = \gamma_0 - (\alpha\Gamma_1 + \beta\Gamma_2)$, where γ_0 is the interfacial tension without a surfactant and both α and β are positive constants. Assuming the shorter relaxation time of fluid dynamics rather than that of chemical dynamics at the interface, we consider the fluid as in a steady state induced by the flow at the interface of the droplet (Marangoni flow). As we are interested in the dynamics near the critical point of the drift bifurcation, we assume low-Reynolds hydrodynamics. In this condition, the steady flow can be obtained as a solution of the Stokes equation with the interfacial tension gradient as the boundary condition [35] (see the Supplemental Material for advection velocity [36]).

Numerical simulations are performed using polar coordinates for an axisymmetric two-dimensional system. Under the above assumptions, our modified model is expressed as

$$\frac{\partial \Gamma_1}{\partial t} + v_\theta(R, \theta)\frac{1}{R}\frac{\partial \Gamma_1}{\partial \theta} = D_s \frac{1}{R^2}\frac{\partial^2 \Gamma_1}{\partial \theta^2} - \kappa_2 \Gamma_1 + D\frac{\partial c}{\partial r}\bigg|_{r=R},$$
(1)

$$\frac{\partial \Gamma_2}{\partial t} + v_\theta(R, \theta)\frac{1}{R}\frac{\partial \Gamma_2}{\partial \theta} = D_s \frac{1}{R^2}\frac{\partial^2 \Gamma_2}{\partial \theta^2} + \kappa_2 \Gamma_1 - \kappa_d \Gamma_2, \quad (2)$$

$$\frac{\partial c}{\partial t} + \vec{v} \cdot \vec{\nabla} c = D\nabla^2 c - \kappa(c - c_\infty), \quad (3)$$

where $(1/R)\partial/\partial\theta$ is the surface derivative for a sphere, and κ_d represents the desorption rate of the product. κ is the relaxation rate of the reactant concentration in the bulk, and c_∞ is the concentration of the surfactant far from the droplet. The boundary condition for the bulk is the Dirichlet condition $c(r_\infty) = c_\infty$, where r_∞ indicates the distance far from the interface, and the linear relation with Henry's constant κ_H at the interface is $\kappa_H c(R, \theta) = \Gamma_1(\theta)$. Because of the linear relation between the interfacial tension and the concentrations of the surfactants,

$$\gamma = \gamma_0 - (\alpha + \beta)[(1 - \rho)\Gamma_1 + \rho\Gamma_2], \quad (4)$$

where we set $\rho = \beta/(\alpha + \beta)$. Here, in the case of $\rho > 0.5$, the product decreases the interfacial tension more than the reactant. It means that the chemical reaction of the surfactant significantly decreases the interfacial tension. In contrast, with $\rho < 0.5$, the interfacial tension of the O/W interface with the reactant is much smaller than that with the product. Hereafter, we will refer the former case as a "decrease of interfacial tension after the chemical reaction" and the latter as an "increase

of interfacial tension after the chemical reaction." In both cases, the interfacial tension γ with a surfactant is smaller than that of pure interface γ_0, because the surfactant must decrease the interfacial tension. In other words, we consider only the positive values of α and β in this paper.

Let us normalize Eqs. (1)–(3) with dimensionless variables $\tilde{\Gamma}_i = (\sqrt{D/\kappa}/c_\infty)\Gamma_i$, $\tilde{c} = c/c_\infty$, $\tilde{t} = \kappa t$, $\tilde{r} = \sqrt{\kappa/D}r$, and $\tilde{\vec{v}} = \vec{v}/\sqrt{D\kappa}$ as

$$\frac{\partial \tilde{\Gamma}_1}{\partial \tilde{t}} + \frac{\tilde{v}_\theta}{\tilde{R}}\frac{\partial \tilde{\Gamma}_1}{\partial \theta} = \frac{\tilde{D}}{\tilde{R}^2}\frac{\partial^2 \tilde{\Gamma}_1}{\partial \theta^2} - K_2\tilde{\Gamma}_1 + \frac{\partial \tilde{c}}{\partial \tilde{r}}, \quad (5)$$

$$\frac{\partial \tilde{\Gamma}_2}{\partial \tilde{t}} + \frac{\tilde{v}_\theta}{\tilde{R}}\frac{\partial \tilde{\Gamma}_2}{\partial \theta} = \frac{\tilde{D}}{\tilde{R}^2}\frac{\partial^2 \tilde{\Gamma}_2}{\partial \theta^2} + K_2\tilde{\Gamma}_1 - K_1\tilde{\Gamma}_2, \quad (6)$$

$$\frac{\partial \tilde{c}}{\partial \tilde{t}} + \tilde{\vec{v}} \cdot \tilde{\nabla}\tilde{c} = \tilde{\nabla}^2\tilde{c} + 1 - \tilde{c}, \quad (7)$$

where $K_1 = \kappa_d/\kappa$, $K_2 = \kappa_2/\kappa$, $\tilde{R} = R\sqrt{\kappa/D}$, and $\tilde{D} = D_s/D$. We also normalize the boundary conditions with constant $K_H = \kappa_H\sqrt{\kappa/D}$ as

$$\tilde{c}(\tilde{r}_\infty) = 1, \quad K_H\tilde{c}(\tilde{R}, \theta) = \tilde{\Gamma}_1(\theta), \quad (8)$$

and advection velocity as

$$\tilde{v}_r^{(o)} = -\tilde{v}_0\sum_{m=1}^\infty \frac{m}{2}\left[\left(\frac{\tilde{R}}{\tilde{r}}\right)^{m-1} - \left(\frac{\tilde{R}}{\tilde{r}}\right)^{m+1}\right]$$
$$\times (\tilde{\Gamma}_m^c\cos m\theta + \tilde{\Gamma}_m^s\sin m\theta), \quad (9)$$

$$\tilde{v}_r^{(i)} = -\tilde{v}_0\sum_{m=1}^\infty \frac{m}{2}\left[\left(\frac{\tilde{r}}{\tilde{R}}\right)^{m+1} - \left(\frac{\tilde{r}}{\tilde{R}}\right)^{m-1}\right]$$
$$\times (\tilde{\Gamma}_m^c\cos m\theta + \tilde{\Gamma}_m^s\sin m\theta), \quad (10)$$

$$\tilde{v}_\theta^{(o)} = -\tilde{v}_0\sum_{m=1}^\infty \frac{1}{2}\left[(m-2)\left(\frac{\tilde{R}}{\tilde{r}}\right)^{m-1} - m\left(\frac{\tilde{R}}{\tilde{r}}\right)^{m+1}\right]$$
$$\times (\tilde{\Gamma}_m^c\sin m\theta - \tilde{\Gamma}_m^s\cos m\theta) + \tilde{v}_0\frac{\tilde{r}_0}{\tilde{R}}\sum_{m=1}^\infty \tilde{\Gamma}_m^s, \quad (11)$$

$$\tilde{v}_\theta^{(i)} = -\tilde{v}_0\sum_{m=1}^\infty \frac{1}{2}\left[-(m+2)\left(\frac{\tilde{r}}{\tilde{R}}\right)^{m+1} + m\left(\frac{\tilde{r}}{\tilde{R}}\right)^{m-1}\right]$$
$$\times (\tilde{\Gamma}_m^c\sin m\theta - \tilde{\Gamma}_m^s\cos m\theta) + \tilde{v}_0\frac{\tilde{r}}{\tilde{R}}\sum_{m=1}^\infty \tilde{\Gamma}_m^s, \quad (12)$$

where

$$\tilde{\Gamma}_m^c = \int_0^{2\pi} [(1-\rho)\tilde{\Gamma}_1 + \rho\tilde{\Gamma}_2]\cos m\theta\, d\theta, \quad (13)$$

$$\tilde{\Gamma}_m^s = \int_0^{2\pi} [(1-\rho)\tilde{\Gamma}_1 + \rho\tilde{\Gamma}_2]\sin m\theta\, d\theta, \quad (14)$$

$$\tilde{v}_0 = \frac{(\alpha + \beta)c_\infty}{2\pi(\eta_i + \eta_o)\kappa}. \quad (15)$$

Here $\tilde{v}_0$ is a function of inverse proportional to viscosity, that is, $\tilde{v}_0$ represents the mobility of bulk.

B. Results

We assume that the relaxation rate of the reactant in the bulk κ is significantly faster than the desorption rate of the
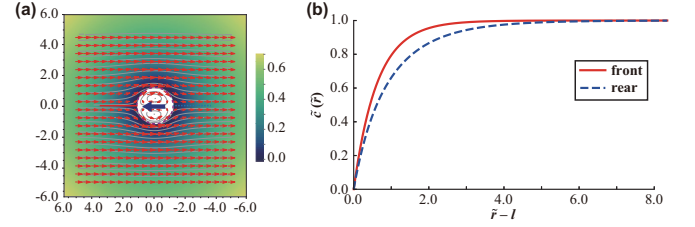

FIG. 1. (a) Typical example of the concentration field $\tilde{c}(\tilde{r}, \theta)$ (color map) and stream line (red arrows). A white circle at the center indicates the droplet, and a blue arrow in the circle indicates the direction of motion. (b) Surfactant profile in the bulk $\tilde{c}(\tilde{r})$. The red solid line shows the concentration at the front [along the red solid line in (a)], and the blue broken line shows that at the rear [along the blue broken line in (a)]. Data were obtained from $\rho = 0.7$, $\tilde{v}_0 = 5$.

product κ_d, $K_1 = 0.01$, and the reaction rate κ_2, $K_2 = 0.1$. Moreover, the diffusion in the bulk D is faster than that on the interface D_s, $\tilde{D} = 0.1$, and Henry's constant $K_H = 10^2$. The initial conditions are given as $\tilde{c}(\tilde{r}, \theta) = 1$, $\tilde{\Gamma}_1(\theta) = 0.01(1 - \cos\theta)$, and $\tilde{\Gamma}_2(\theta) = 0$. Because we want to understand fundamental mechanism of the translational motion, we consider only the simplest case, $m = 1$, in the advection velocity. Note that with the higher order solution, a variety of motions such as rotational or oscillational motion are reported in previous models [32,35]. The above parameters are fixed as constants through the simulation.

Initially, to verify our model, we make numerical calculations with $\rho = 0$, which means the product has no effect on the interfacial tension. This situation corresponds to the Yoshinaga model [33]. As with the previous report [33], the bifurcation from no motion to continuous motion occurs with changing bifurcation parameter $\tilde{v}_0$ (see Fig. S1 in the Supplemental Material [36]). As the dynamics of a droplet are enhanced by momentum conservation for hydrodynamics, the maximum speed of the fluid at the interface $\tilde{v}_d = \max \tilde{v}_\theta(\tilde{R}, \theta)$ is regarded as the speed of the droplet. Above the critical value, $\tilde{v}_d$ increases with $\tilde{v}_0$. Hereafter, we set $\tilde{v}_0 = 5$, which is sufficiently large to observe the droplet motion.

Next, we consider the situation $\rho = 0.7$, in which the product rather than the reactant decreases the interfacial tension. Figure 1 shows the concentration field $\tilde{c}(\tilde{r}, \theta)$ and the velocity field $\tilde{\vec{v}}(\tilde{r}, \theta)$ near the droplet in the steady state. Due to momentum conservation, the droplet moves from right to left in Fig. 1(a). There is a certain difference between the concentration in the direction of motion (front) and that in the opposite direction (rear). In Fig. 1(b), $\tilde{c}(\tilde{r})$ has a steeper gradient at the front than at the rear. In addition, both concentrations, $\tilde{\Gamma}_1$ and $\tilde{\Gamma}_2$, have their maximum values at the front and their minimum values at the rear. These inhomogeneous distributions lead to a spatial gradient of interfacial tension and consequently Marangoni flow; thus, the droplet starts to move.

Here we consider the effect of the activity of surfactants at the interface ρ and the reaction rate K_2 on the droplet motion. The ρ dependency of the droplet speed $\tilde{v}_d$ is shown in Fig. 2(a) for different values of K_2. The value of $\tilde{v}_d$ decreases as the activity of the products increases at low values of K_2. In contrast, the relation between $\tilde{v}_d$ and ρ is reversed
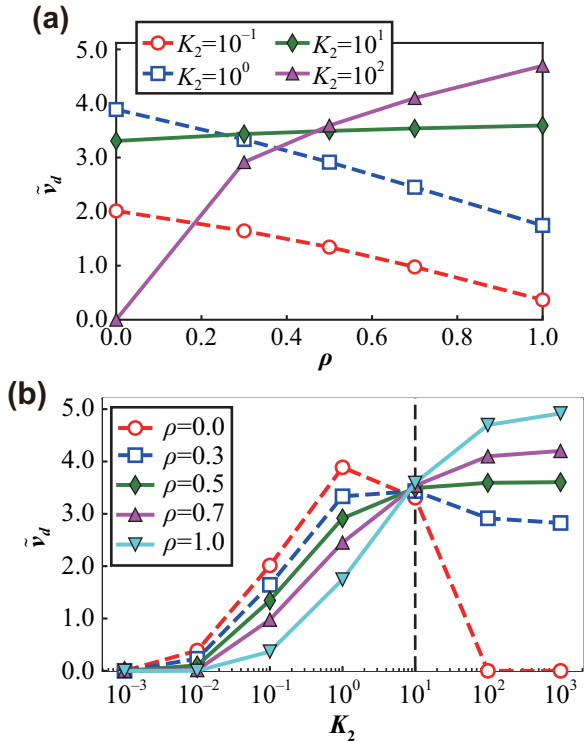
FIG. 2. (a) Droplet speed $\tilde{v}_d$ dependence on ρ for lower K_2 (broken lines with open symbols) and higher K_2 (solid lines with filled symbols). (b) Droplet speed $\tilde{v}_d$ against K_2 with various ρ. Broken lines with open symbols indicate $\beta < 0.5$, and solid lines with filled symbols indicate $\rho \geqslant 0.5$. Dashed vertical line indicates $K_2^c \sim 10$.

for high values of K_2; positive correlations between $\tilde{v}_d$ and ρ are observed. The same data are replotted against K_2 in Fig. 2(b). The K_2 dependency of $\tilde{v}_d$ depends on the value of ρ; $\tilde{v}_d$ has a peak at approximately $K_2 = 1$ for $\rho < 0.5$, whereas $\tilde{v}_d$ monotonically increases with the value of K_2 for $\rho > 0.5$. This monotonic increase is due to compensation of the decrease of the interfacial tension by the reactant. Although at higher K_2, the concentration of the reactant Γ_1 decreases because of saturation of the reaction and that of the product Γ_2 increases, and it causes a further decrease of the interfacial tension at the front. In addition, for all values of ρ, the droplet does not move in the low-K_2 region and $\tilde{v}_d$ appears to plateau in the high-K_2 region. The lack of motion at a negligible reaction rate $K_2 = 10^{-3}$ indicates that the chemical reaction is required for droplet motion. As shown in Fig. 2(a), the negative correlation between $\tilde{v}_d$ and ρ turns into a positive one at the crossing point $K_2^c \sim 10$ [Fig. 2(b)], where the value of speed $\tilde{v}_d$ is independent of ρ. Here the amounts of the surfactants at the interface, $\tilde{\Gamma}_1$ and $\tilde{\Gamma}_2$, are key factors because the velocity of the surrounding fluid is calculated as a function of them in our model.

Because Marangoni flow is originally caused by the chemical gradients, the simple approximation of the chemical gradient $\Delta \tilde{\Gamma} = \max \tilde{\Gamma} - \min \tilde{\Gamma}$ is an effective way of discussing the droplet motion. The gradient of the reactant $\Delta \tilde{\Gamma}_1$ against K_2 has a peak around $K_2 = 1$, and that of the product $\Delta \tilde{\Gamma}_2$ monotonically increases with the value of K_2 except for at

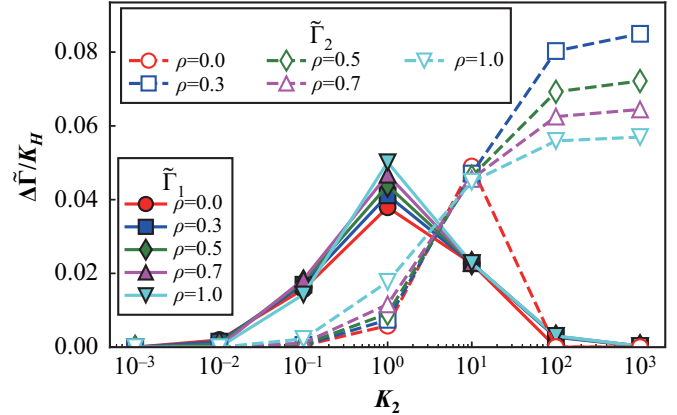FIG. 3. Differences between the maximum and minimum values of surfactants at the interface, $\Delta \Gamma_1$ (filled symbols with solid lines) and $\Delta \Gamma_2$ (open symbols with broken lines), against K_2 for various values of ρ.

$\rho = 0$ (Fig. 3). With K_2 smaller than the critical value, $\Delta \tilde{\Gamma}_1$ is larger than $\Delta \tilde{\Gamma}_2$, and the relationship is reversed with the value of K_2 overcoming the critical one. This critical value is of the same order as the crossing point K_2^c [Fig. 2(b)]. Moreover, $\Delta \tilde{\Gamma}_1$ and $\tilde{v}_d$ seem to have peaks at similar values of K_2 for $\rho < 0.5$, where the reactant plays a more important role for decreasing the interfacial tension than the product. In contrast, $\tilde{v}_d$ monotonically increases with K_2 for $\rho > 0.5$. These results indicate that the droplet speed is determined by the interfacial chemical gradient. In addition, the plateau region for high values of K_2 can also be explained in terms of the chemical gradient as follows. For high values of K_2, almost all reactant molecules on the interface immediately change to the product, and the amount of reactant is restricted by the adsorption rate. This is how the value of max $\tilde{\Gamma}_2$ is limited, and it confines the gradient to a finite value. It should be mentioned that the amount of product desorbed from the interface into the bulk cannot be ignored in the higher K_2 region; hence, we should consider the concentration of the product in the bulk. Note that, in the cases of $K_2 \geqslant 10^2$ with $\rho = 0$ or $K_2 \leqslant 10^{-3}$ with any value of ρ, no chemical gradient $\Delta \tilde{\Gamma}_i = 0$ ($i = 1, 2$) causes any motion of the droplet. Isotropic distribution of the surfactant around the droplet is developed in these situations.

We also investigated the dependence of droplet speed $\tilde{v}_d$ on the desorption rate K_1 and diffusion on an interface $\tilde{D}$. Except for $K_1 \geqslant 10^1$ with $\rho = 1$ and $\tilde{D} \geqslant 1$ with any value of ρ, for which the droplet does not move, these parameters have less effect on $\tilde{v}_d$.

III. EXPERIMENTS

A. Material and method

1-Oleoyl-rac-glycerol (monoolein, MO; purity $>$ 99%) was purchased from Sigma-Aldrich and used without further purification. Water was purified using a Milli-Q system (Ultrapure Water Direct-Q 3UV, Merck). MO was dissolved in squalane (10 mM), and the solution was used as the oil phase. The aqueous phase was a mixture of sodium bromate (0.4 M) and sulfuric acid (0.0–1.8 M), with ferroin (4.0 mM) as a
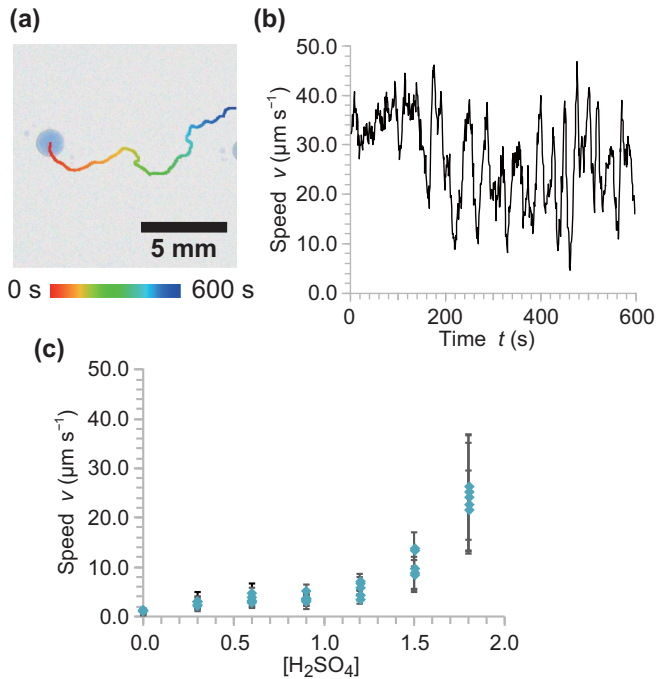
FIG. 4. (a) Trajectory of the droplet motion. The aqueous droplet is composed of BrO_3^- (0.4 M) and H_2SO_4 (1.8 M). The color of the trajectory indicates the time. (b) Time series of speed. (c) Average speed of droplet motion as a function of concentration of H_2SO_4. The error bars indicate standard deviation of speed in time.

redox indicator. An aqueous droplet (0.2 μl) was prepared and added into the oil phase using a micropipette. Droplet motion was monitored using an optical microscope (Nikon, SMZ1000, frame rate 1 fps).

B. Results

The aqueous droplet, which is composed of BrO_3^- and H_2SO_4, spontaneously moved with almost constant speed in a monoolein-squalane solution [Figs. 4(a) and 4(b)]. The speed of the droplet increased with an increase in the H_2SO_4 concentration in the aqueous droplet [Fig. 4(c)]. When [H_2SO_4] = 0.0 M, the droplet speed was almost 1 μm s^{-1}, which was slow but much faster than the fluctuation (Brownian motion) of a droplet of 1 mm diameter. The speed gradually increased with [H_2SO_4] up to 0.9 M and drastically increased over 0.9 M. In the strong acidic condition, the decomposition process of the BrO_3^- is accelerated, and, in consequence, the brominated MO becomes abundant at the interface. Therefore, we regard the concentration of H_2SO_4 as a kind of accelerator of reaction rate. Note that with high concentration of H_2SO_4 in droplets, fluctuation also drastically increased.

IV. DISCUSSION

In the experiments, H_2SO_4 and BrO_3^- produce Br_2 in the aqueous phase. In the presence of Br_2, the α bromination of carbonyl compounds of the MO occurs in a highly acidic solution, and the reaction rate is proportional to the concen-

tration of H_2SO_4 [34]. It means that κ_2 is proportional to the concentration of H_2SO_4. The concentration of MO in the bulk is represented as c in our model, and surface concentration of MO and brominated MO on the droplet correspond to Γ_1 and Γ_2, respectively. Our observation suggests that a higher reaction rate induces faster droplet motion [Fig. 4(c)].

Let us compare the numerical results with the experimental observations to validate our model. As shown previously, our droplet moves even in the case of $\rho > 0.5$. This condition corresponds to the decrease in interfacial tension after the chemical reaction. In the experiments, with the increase in the concentration of H_2SO_4, the droplet speed also increases [Fig. 4(c)]. According to the previous experimental report [34], we obtain $K_2/K_1 = \kappa_2/\kappa_d \approx 10[H_2SO_4]$, and $\rho = 0.75$; that is, the increase in concentration of H_2SO_4 causes an increase in the reaction rate K_2. In our model, the droplet speed monotonically increases with reaction rate K_2 for $\rho > 0.5$ (see also magenta triangles with solid line in Fig. 2(b)), which shows good agreement with the experiments.

Moreover, this K_2 dependency can be applied to the pH-dependent motion of a nitrobenzene droplet including DHEPA [29]. The droplet spontaneously moves in the high-pH aqueous phase, which enhances deprotonation. In the high-pH condition, deprotonated DEHPA becomes rich at the interface, and only deprotonated DEHPA decreases the interfacial tension. Namely, the droplet dynamics drastically change from immobile to spontaneous swimming with increasing pH, which corresponds to Fig. 2(b) in the case of $\rho \sim 1$.

In addition, the effect of droplet size on the swimming speed is also confirmed in our model. There is a peak in the droplet speed $\tilde{v}_d$ for the radius $\tilde{R}$ at any value of ρ (see Fig. S2 in the Supplemental Material [36]). This result corresponds to the theoretical analysis in the Yoshinaga model [33]. In previous experimental reports, the larger droplets swam faster in the bulk [29,37]; the droplet in our model also becomes faster with increasing $\tilde{R}$ below the peak. These agreements support the validity of our model.

We should mention the amounts of surfactants at the interface. Here we consider the dominant species at the interface: the reactant and product. For rough estimation, we ignore the spatial gradient of the surfactants at the interface; this is a reasonable assumption because the value of $\Delta\tilde{\Gamma}$ is much smaller than that of $\tilde{\Gamma}$. Under the assumption of a homogeneous distribution, the ratio of $\tilde{\Gamma}_1$ and $\tilde{\Gamma}_2$ in steady states can be easily obtained from Eq. (6) as (max $\tilde{\Gamma}_1$/ max $\tilde{\Gamma}_2$) $\approx$ (K_1/K_2). This rough estimation is verified by the results of the numerical calculations (see Fig. S3 in the Supplemental Material [36]). This means that the reactant is dominant at low values of K_2, but the product shifts to become the dominant species with increasing K_2. The dominant species can approximately explain the ρ dependency of $\tilde{v}_d$, as shown in Fig. 2(a), although it should be emphasized that it is inadequate because negative correlation is still observed for $K_2 = 10^{-1}$, whereas the dominant surfactant has already reversed at $K_1 = K_2 = 10^{-2}$. Note that it takes significantly longer to achieve the steady states of maximum values max $\tilde{\Gamma}$ than those of chemical gradients $\Delta\tilde{\Gamma}$ and advection velocity $\vec{v}$.

Here we discuss the mechanism of a swimming droplet in bulk (Fig. 5). The key factor in the droplet dynamics
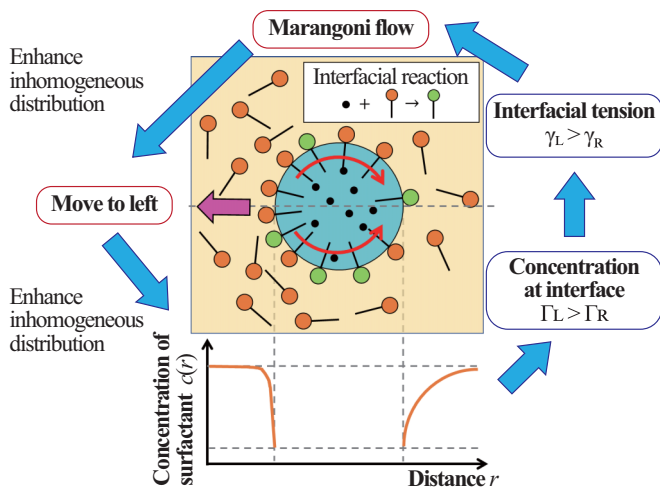
FIG. 5. Schematic illustration of the mechanism of droplet motion.

is the gradient of the bulk concentration of surfactant. The initial fluctuation of the surfactant concentrations in the bulk induces similar fluctuation at the interface and leads to inhomogeneous interfacial tension, resulting in Marangoni flow. Due to Marangoni flow and momentum conservation, the droplet moves to the region of higher surfactant concentration. The concentration of the surfactant at the interface becomes slightly higher at the front than at the rear, therefore enhancing the inhomogeneous distribution of the surfactant further. Namely, a positive feedback appears between the concentration gradients and the droplet motion. This mechanism does not conflict with the previously proposed ones [34,35].

In the previous models, the increase in interfacial tension after the chemical reaction was necessary for continuous droplet motion [28,32,33]. However, as shown by experimental results [29,34], a droplet potentially shows spontaneous motion when the interfacial tension decreases after the chemical reaction. As shown above, the droplet moves even in the case of $\rho > 0.5$, which corresponds to a decrease in interfacial tension after the chemical reaction. These results indicate that the droplet motion is unaffected by whether the interfacial tension increases or decreases.

V. CONCLUSION

In this paper, we constructed an improved model for spontaneous droplet motion in bulk to explain the experimental observations in which the interfacial tension decreases after the chemical reaction at the interface. We considered the concentration of two kinds of chemical species on the interface, reactant and product, and the reactant in the bulk. This model enables us to discuss the effect of the product activity on the interfacial tension. By varying the ratio of activity of the reactant and product, ρ, we revealed that the droplet potentially moves under any value of ρ. In addition, the droplet speed monotonically increases with reaction rate K_2 when $\rho > 0.5$, which agrees with experimental results [29,34]. Because our motivation is to construct such an improved model, we only considered the simplest case of the solution with $m = 1$ in Eqs. (9)–(12). As mentioned above, the higher order solution $m > 1$ causes bifurcation of a droplet motion, e.g., rotation [32,35]. To evaluate the contribution of the bifurcation of the droplet motion due to a higher order solution is future work. Although the phenomenological explanation of the droplet motion is similar to the previously proposed one [33], our results indicate that it makes no difference to the droplet motion whether the interfacial tension increases or decreases with chemical reaction of the surfactant. This nondependency allows the restriction of droplet motion that was required in previous models to be relaxed [28,32,33]. We expect this moderation of the requirement to provide an explanation for the droplet dynamics in various kinds of experimental systems. In addition, the droplet system shows similarity to other self-propelled systems, e.g. a droplet or disk sliding on a water surface, from the perspective of the dynamical mechanism. Namely, the droplet motion occurs via the coupling of the bulk concentration profile and its movement.

[1] D. A. Bratsun and A. De Wit, On Marangoni convective patterns driven by an exothermic chemical reaction in two-layer systems, Phys. Fluids **16**, 1082 (2004).

[2] K. Eckert, M. Acker, R. Tadmouri, and V. Pimienta, Chemo-Marangoni convection driven by an interfacial reaction: Pattern formation and kinetics, Chaos **22**, 037112 (2012).

[3] K. Eckert and A. Grahn, Plume and Finger Regimes Driven by an Exothermic Interfacial Reaction, Phys. Rev. Lett. **82**, 4436 (1999).

[4] T. Banno and T. Toyota, Molecular system for the division of self-propelled oil droplets by component feeding, Langmuir **31**, 6943 (2015).

[5] S. Hussein, J. Maselko, and J. T. Pantaleone, Growing a chemical garden at the air-fluid interface, Langmuir **32**, 706 (2016).

[6] S. Nakata, M. Nagayama, H. Kitahata, N. J. Suematsu, and T. Hasegawa, Physicochemical design and analysis of self-propelled objects that are characteristically sensitive to environments, Phys. Chem. Chem. Phys. **17**, 10326 (2015).

[7] N. J. Suematsu and S. Nakata, Evolution of self-propelled objects: From the viewpoint of nonlinear science, Chem. Eur. J. **24**, 6308 (2018).

[8] Y. Hong, D. Velegol, N. Chaturvedi, and A. Sen, Biomimetic behavior of synthetic particles: From microscopic randomness to macroscopic control, Phys. Chem. Chem. Phys. **12**, 1423 (2010).

[9] W. F. Paxton, S. Sundararajan, T. E. Mallouk, and A. Sen, Chemical locomotion, Angew. Chem., Int. Ed. **45**, 5420 (2006).

[10] S. J. Ebbens and J. R. Howse, In pursuit of propulsion at the nanoscale, Soft Matter **6**, 726 (2010).

[11] Y. Cui, D. Li, and H. Bai, Bioinspired smart materials for directional liquid transport, Ind. Eng. Chem. Res. **56**, 4887 (2017).

[12] M. Nagayama, S. Nakata, Y. Doi, and Y. Hayashima, A theoretical and experimental study on the unidirectional motion of a camphor disk, Physica D **194**, 151 (2004).

[13] K. Nagai, Y. Sumino, H. Kitahata, and K. Yoshikawa, Mode selection in the spontaneous motion of an alcohol droplet, Phys. Rev. E **71**, 065301(R) (2005).

[14] C. M. Bates, F. Stevens, S. C. Langford, and J. T. Dickinson, Motion and dissolution of drops of sparingly soluble alcohols on water, Langmuir **24**, 7193 (2008).

[15] I. Lagzi, S. Soh, P. J. Wesson, K. P. Browne, and B. A. Grzybowski, Maze solving by chemotactic droplets, J. Am. Chem. Soc. **132**, 1198 (2010).

[16] T. Bánsági Jr., M. M. Wrobel, S. K. Scott, and A. F. Taylor, Motion and interaction of aspirin crystals at aqueous-air interfaces, J. Phys. Chem. B **117**, 13572 (2013).

[17] N. J. Cira, A. Benusiglio, and M. Prakash, Vapour-mediated sensing and motility in two-component droplets, Nature (London) **519**, 446 (2015).

[18] J. E. Satterwhite-Warden, D. K. Kondepudi, J. A. Dixon, and J. F. Rusling, Co-operative motion of multiple benzoquinone disks at the air-water interface, Phys. Chem. Chem. Phys. **17**, 29891 (2015).

[19] F. Wodlei, J. Sebilleau, J. Magnaudet, and V. Pimienta, Marangoni-driven flower-like patterning of an evaporating drop spreading on a liquid substrate, Nat. Commun. **9**, 820 (2018).

[20] F. Domingues Dos Santos and T. Ondarçuhu, Free-Running Droplets, Phys. Rev. Lett. **75**, 2972 (1995).

[21] Y. Sumino, N. Magome, T. Hamada, and K. Yoshikawa, Self-Running Droplet: Emergence of Regular Motion from Nonequilibrium Noise, Phys. Rev. Lett. **94**, 068301 (2005).

[22] S. Nakanishi, T. Nagai, D. Ihara, and Y. Nakato, Self-propelled oil droplets on metal surfaces during electrodeposition, ChemPhysChem **9**, 2302 (2008).

[23] B. Nanzai, M. Kato, and M. Igawa, Spontaneous motion of various oil droplets in aqueous solution of trimethyl alkyl ammonium with different carbon chain lengths, Colloids Surf. A **504**, 154 (2016).

[24] X. Yao, H. Bai, J. Ju, D. Zhou, J. Li, H. Zhang, B. Yang, and L. Jiang, Running droplet of interfacial chemical reaction flow, Soft Matter **8**, 5988 (2012).

[25] K. John, M. Bär, and U. Thiele, Self-propelled running droplets on solid substrates driven by chemical reactions, Eur. Phys. J. E **18**, 183 (2005).

[26] M. M. Hanczyc, T. Toyota, T. Ikegami, N. Packard, and T. Sugawara, Fatty acid chemistry at the oil-water interface: Self-propelled oil droplets, J. Am. Chem. Soc. **129**, 9386 (2007).

[27] T. Toyota, N. Maru, M. M. Hanczyc, T. Ikegami, and T. Sugawara, Self-propelled oil droplets consuming "Fuel" surfactant, J. Am. Chem. Soc. **131**, 5012 (2009).

[28] S. Thutupalli, R. Seemann, and S. Herminghaus, Swarming behavior of simple model squirmers, New J. Phys. **13**, 073021 (2011).

[29] T. Ban, T. Yamagami, H. Nakata, and Y. Okano, pH-dependent motion of self-propelled droplets due to Marangoni effect at neutral pH, Langmuir **29**, 2554 (2013).

[30] S. Miura, T. Banno, T. Tonooka, T. Osaki, S. Takeuchi, and T. Toyota, pH-induced motion control of self-propelled oil droplets using a hydrolyzable gemini cationic surfactant, Langmuir **30**, 7977 (2014).

[31] C. Jin, C. Krüger, and C. C. Maass, Chemotaxis and autochemotaxis of self-propelling droplet swimmers, Proc. Natl. Acad. Sci. USA **114**, 5089 (2017).

[32] M. Schmitt and H. Stark, Swimming active droplet: A theoretical analysis, Europhys. Lett. **101**, 44008 (2013).

[33] N. Yoshinaga, K. H. Nagai, Y. Sumino, and H. Kitahata, Drift instability in the motion of a fluid droplet with a chemically reactive surface driven by Marangoni flow, Phys. Rev. E **86**, 016108 (2012).

[34] N. J. Suematsu, K. Saikusa, T. Nagata, and S. Izumi, Interfacial dynamics in the spontaneous motion of an aqueous droplet, Langmuir **35**, 11601 (2019).

[35] K. H. Nagai, F. Takabatake, Y. Sumino, H. Kitahata, M. Ichikawa, and N. Yoshinaga, Rotational motion of a droplet induced by interfacial tension, Phys. Rev. E **87**, 013009 (2013).

[36] See Supplemental Material at http://link.aps.org/supplemental/10.1103/PhysRevE.102.023102 for (i) advection velocity, (ii) bifurcation from no motion to continuous motion, (iii) size dependency, and (iv) dominant chemical species at the interface.

[37] N. Ueno, T. Banno, A. Asami, Y. Kazayama, Y. Morimoto, T. Osaki, S. Takeuchi, H. Kitahata, and T. Toyota, Self-propelled motion of monodisperse underwater oil droplets formed by a microfluidic device, Langmuir **33**, 5393 (2017).